Published in final edited form as:
Atmos Environ (1994). 2017 ; 160: 36–45. doi:10.1016/j.atmosenv.2017.04.009.

Persistence of initial conditions in continental scale air quality simulations

Christian Hogrefe[1], **Shawn J. Roselle**[1], **Jesse O. Bash**[1]

[1.] Computational Exposure Division, National Exposure Research Laboratory, U.S. Environmental Protection Agency (EPA), Research Triangle Park, NC 27711, USA

Abstract

This study investigates the effect of initial conditions (IC) for pollutant concentrations in the atmosphere and soil on simulated air quality for two continental-scale Community Multiscale Air Quality (CMAQ) model applications. One of these applications was performed for springtime and the second for summertime. Results show that a spin-up period of ten days commonly used in regional-scale applications may not be sufficient to reduce the effects of initial conditions to less than 1% of seasonally-averaged surface ozone concentrations everywhere while 20 days were found to be sufficient for the entire domain for the spring case and almost the entire domain for the summer case. For the summer case, differences were found to persist longer aloft due to circulation of air masses and even a spin-up period of 30 days was not sufficient to reduce the effects of ICs to less than 1% of seasonally-averaged layer 34 ozone concentrations over the southwestern portion of the modeling domain. Analysis of the effect of soil initial conditions for the CMAQ bidirectional NH_3 exchange model shows that during springtime they can have an important effect on simulated inorganic aerosols concentrations for time periods of one month or longer. The effects are less pronounced during other seasons. The results, while specific to the modeling domain and time periods simulated here, suggest that modeling protocols need to be scrutinized for a given application and that it cannot be assumed that commonly-used spin-up periods are necessarily sufficient to reduce the effects of initial conditions on model results to an acceptable level. What constitutes an acceptable level of difference cannot be generalized and will depend on the particular application, time period and species of interest. Moreover, as the application of air quality models is being expanded to cover larger geographical domains and as these models are increasingly being coupled with other modeling systems to better represent air-surface-water exchanges, the effects of model initialization in such applications needs to be studied in future work.

Keywords

Initial conditions; spin-up period; soil concentrations; inert tracers

---

1 Introduction

Eulerian air quality modeling systems used in research, forecasting, and air quality planning applications simulate atmospheric pollutant concentrations through the numerical representation of emissions, transport, transformation, and removal processes affecting pollutant concentrations. These models require the specification of initial and lateral boundary conditions. Ideally, these initial and boundary conditions would be based on observations, but in reality, this is not feasible due to the large number of species and extensive spatial domains handled by these models. Therefore, initial concentrations are often based on estimated climatological conditions (Byun and Schere, 2006) or global scale models while lateral boundary conditions often are derived from global scale models (Schere et al., 2012). Studying the effect of boundary conditions on regional air quality simulations continues to be a topic of active research interest due to the need to properly quantify large-scale background concentrations and intercontinental transport in regional applications (e.g. Schere et al., 2012; Dolwick et al., 2015; Giordano et al., 2015). On the other hand, little recent work has been performed to quantify the impact of initial conditions on simulated concentrations. While it is a generally accepted practice to “spin up” a model for a certain time period prior to the study period of interest to reduce or eliminate the effects of initial conditions, to our best knowledge no recent studies have been performed to quantify the necessary time periods for continental-scale applications. In the earlier days of regional air quality modeling, Brost (1988) performed sensitivity simulations with the Regional Acid Deposition Model (RADM) (Chang et al., 1987) and found that the effects of initial conditions on key reactive species became insignificant after a 2–3 day spin-up period for a domain covering 2,400 by 2,400 km. Berge et al. (2001) performed simulations with both a box model and regional air quality model for a domain over the San Joaquin Valley and found that, within the planetary boundary layer, the impact of initial conditions falls to < 10% after 48 hours with the exception of PAN and HNO_3 at some locations. For the free troposphere, they found that impacts >10% were seen for reservoir species even after three days spin-up over larger portions of the domain. Over the following decade, a number of regional scale air quality applications used a spin-up period of three days (Sistla et al., 2001; Tao et al., 2003; Hogrefe et al., 2004; Foley et al., 2010). With the increasing number of model applications encompassing the entire conterminous U.S., spin-up periods were extended to ten days (Appel et al., 2010; Appel et al., 2012; Hogrefe et al., 2015); however, no formal analysis was presented in these studies to demonstrate that the increased spin-up period was sufficient to eliminate the effects of initial conditions.

In addition to applications at increasingly large domains, air quality modeling systems have also become more complex, integrating more interactions between the atmosphere and land surface, in part through coupling with other models. One example is the treatment of bidirectional NH_3 air/surface exchange implemented in the Community Multiscale Air Quality (CMAQ) model (Byun and Schere, 2006) as described in Bash et al. (2010, 2013) and Pleim et al. (2013). By including such interactions, the question of how model initialization affects simulated concentrations potentially needs to be expanded beyond the traditional focus on atmospheric initial conditions to include initial conditions in other media such as concentrations in the soil. The present study addresses both the persistence of atmospheric initial conditions for continental-scale applications and the persistence of soil initial condition effects in CMAQ applications using the bidirectional NH_3 flux approach.

2 Model Simulations

The regional air quality simulations analyzed in this study were performed with version 5.0.2 of CMAQ. Meteorological fields were prepared using version 3.4 of the Weather Research and Forecasting (WRF) model (Skamarock and Klemp, 2007). Throughout the WRF simulation, nudging of temperature, wind speed, and water vapor mixing ratio was applied above the PBL following the approach described in Gilliam et al. (2012). In addition, soil temperature and moisture nudging as described in Pleim and Xiu (2003) and Pleim and Gilliam (2009) was applied as well. The 2010 emission inputs are described in Pouliot et al. (2015). The CMAQ simulations were performed with a horizontal grid spacing of 12 km over the continental U.S. with a vertical extent to 50mb (roughly 20 km above sea level) using 35 vertical layers. Model layer 34 used in some of the analyses presented in Section 3 extends roughly from 13.8 km to 16.2 km above sea level. Chemical boundary conditions were prepared from global concentration fields simulated by the European Center for Medium Range Weather Forecasts (ECMWF) Composition – Integrated Forecast System (C-IFS) model (Flemming et al., 2015). Additional details on the configuration of WRF and CMAQ can be found in Solazzo et al. (2017). Four sets of simulations were performed to study the effects of initial conditions on simulated air quality. The first simulation, serving as reference simulation and hereafter referred to as BASE, was initialized on December 22, 2009 and run continuously to August 31, 2010. The second simulation, hereafter referred to as SPRING_PROF, was initialized on February 23, 2010 and run to April 30, 2010. The third and fourth simulations, hereafter referred to as SUMMER_PROF and SUMMER_CIFS, were initialized on June 21, 2010 and run to August 31, 2010. By contrasting the results from the sensitivity simulations (i.e. SPRING_PROF, SUMMER_PROF, and SUMMER_CIFS) with the results from the BASE simulation, the effects and persistence of model initialization could be studied for 67 days in spring and 72 days in summer. In all four simulations, initialization of the bidirectional model for NH_3 relied on NH_4^+ and H^+ concentrations simulated by the Environmental Policy Integrated Climate (EPIC) model (Williams, 1984; 2012) as described in Cooter et al. (2012), Pleim et al. (2013) and Bash et al. (2013). For the BASE, SPRING_PROF, and SUMMER_PROF simulations, atmospheric concentrations were initialized using the default CMAQ profile summarized for selected species in Table 1. It should be noted that when this default profile was first developed, the top of the model was lower than the 50 mb top used in this study and many other recent applications. For the SUMMER_CIFS simulation, atmospheric concentrations were initialized from the global C-IFS fields rather than the default CMAQ profile to investigate whether potentially more realistic initial conditions might lead to faster convergence between the base case and sensitivity simulations. A comparison of results from the BASE simulation against observations and other regional-scale model simulations was presented in Solazzo et al. (2017). The SPRING_PROF and SUMMER_PROF simulations included a chemically inert initial condition tracer (hereafter referred to as ICT) that undergoes advection and diffusion but is not affected by chemistry, deposition or scavenging. The ICT mixing ratio was arbitrarily set to 50 ppb at the beginning of the sensitivity simulations throughout the modeling domain and there were no ICT emissions and lateral boundary conditions throughout the simulations. The addition of the ICT in the SPRING_PROF and SUMMER_PROF simulations had no effect on any of the other species simulated by CMAQ.

3 Analysis and Results

3.1 Atmospheric Concentration Initialization

Figures 1a–b show time-height cross sections of domain maximum ICT mixing ratios for the spring and summer cases. As noted above, the ICT mixing ratio was set to 50 ppb throughout the domain at the start of the SPRING_PROF and SUMMER_PROF simulations (February 23, 0 GMT and June 21, 0 GMT). Near the surface, ICT mixing ratios > 30ppb (i.e. 60% of the initial value) can be found after ten days while it takes 25–30 days for mixing ratios to fall to below 0.5 ppb (1% of their initial value). The ICT persistence aloft is similar to the surface results for the summer case but shorter for the spring case when domain maximum mixing ratios drop to less than 0.5 ppb after about 12 days.

The longer persistence of the domain maximum ICT in the upper layers for the summer case suggests the presence of a slow moving circulation pattern. This is confirmed in Figures 2a–d for the spring case and 2e-h for the summer case. Figures 2a–c (e-g) show maps of ICT mixing ratios in model layer 34 (roughly 13.8 km - 16.2 km above sea level) after 10, 20 and 30 days for the spring (summer) cases while figures 2d (h) show maps of the number of days needed for the ICT mixing ratios to drop to below 0.5 ppb (1%) in model layer 34 for the spring (summer) cases. The results for the spring case show that the ICT gets advected to the northeast corner of the modeling domain after 10 days and effectively leaves the modeling domain after fifteen days. In contrast, the results for the summer case show that the ICT is circulated within the modeling domain such that its mixing ratios do not drop below 0.5 ppb (1%) until 25–30 days after the start of the summer simulation over the southwestern portion of the modeling domain.

The analysis of the ICT should be viewed as an upper bound for the persistence of initial conditions since it only accounts for the loss through advection and mixing but does not account for chemical loss, deposition or removal through scavenging. The resulting overestimation is likely most pronounced for lower model layers where chemical transformations, scavenging and deposition are at least as important for the budget of most species as advection and mixing. Conversely, the analysis of the ICT results for the upper layers likely represents a good approximation of the persistence of other species in these layers since their budget is dominated by advection and mixing.

To illustrate the persistence of initial conditions for a reactive species, Figures 3a–c show maps of the number of days needed for differences in ozone mixing ratios between the SPRING_PROF and BASE simulation in model layer 1 to drop to below 1%/5%/10% of the grid-cell specific period-average BASE ozone mixing ratio for the spring simulation (February 23 – April 30). To construct this figure, daily average ozone mixing ratios were computed for each grid cell and each day for the BASE and SPRING_PROF simulations during the February 23 – April 30 time period. Next, the simulation-average BASE mixing ratio was calculated as the mean over these 67 days for the BASE simulation. Finally, absolute differences between SPRING_PROF and BASE were computed for each of the 67 days and divided by the period-average BASE mixing ratio at each grid cell. The maps show the last day (counting from February 23) on which this ratio exceeds 0.01/0.05/0.1 at a given grid cell. Figures 3d–f show the corresponding results for the summertime case (June 21 – August 31) comparing BASE and SUMMER_PROF, and Figures 3g – i show the corresponding results for the summertime case comparing BASE and SUMMER_CIFS. Corresponding results for model layer 34 are shown in Figures 4a–i.

For layer 1, the results indicate that 10 days are sufficient for the ozone differences due to different initializations to drop to below 10% throughout the domain in the spring case and both summer cases and to drop to below 5% throughout the domain in the spring case and the summer case initialized with C-IFS while the summer case initialized with the CMAQ default profiles shows differences greater than 5% for a small portion of the domain. Twenty days are sufficient for the difference to drop to below 1% throughout the domain for the spring case and almost the entire domain except for small areas in Florida and Wisconsin in both summer cases. The differences between panels f) and i) indicate that initializing atmospheric concentrations from the C-IFS global model rather than the CMAQ default profile leads to a faster convergence of surface ozone concentrations between the base case and the sensitivity case.

The findings presented in Figure 3 confirm that the persistence of the ICT shown in Figures 1a–b indeed were an overestimate for the persistence of a reactive species like ozone in the lower model layers. However, the ozone results for layer 34 shown in Figures 4a–f are similar to the corresponding results for the ICT shown in Figures 2a–f, supporting the notion that the ICT results for the upper layers are a good approximation of the persistence of other species in these layers. In addition, the comparison of panels 4d-f to panels 4g-i suggests that initializing atmospheric concentrations with C-IFS does not lead to significantly shorter persistence of the effects of model initialization compared to initializing atmospheric concentrations with the default CMAQ profile. In particular, the spatial mean difference in the persistence between the SUMMER_PROF and SUMMER_CIFS cases for model layer 34 is two days for the 1% and 5% thresholds and four days for the 10% threshold. Figures 4a–c show that for the spring case ozone differences are noticeable only in the northeast corner of the modeling domain after 10 days and not a single grid cell exhibits differences of 1% or greater fifteen days after initialization, consistent with the ICT results in Figures 2a–c. On the other hand, layer 34 ozone differences exceed 1% for more than 30 days over the southwestern portion of the modeling domain for the summer case due to a slow moving circulation pattern for both the SUMMER_PROF and SUMMER_CIFS simulations, again consistent with the with the ICT results in Figures 2d–f.

Tables 2a–c list the results of similar analyses for layer 1 concentrations for a number of additional species. Summarized in these tables are the number and percentage of grid cells where differences due to model initialization exceed 10%/5%/1% of period-mean BASE values for the SPRING_PROF, SUMMER_PROF and SUMMER_CIFS simulations after 10 days (Table 2a), 20 days (Table 2b), and 30 days (Table 2c) of simulations. The species analyzed here are ozone, CO, SO_2, NH_3, PAN, aerosol sulfate, aerosol nitrate, aerosol ammonium, and $PM_{2.5}$ mass. After ten days, differences greater than 1% exist at between 0.8% (O_3, summer initialized with C-IFS) and 68.9% (NH_4^+, spring) of all grid cells for all the species analyzed here, suggesting that a spin-up period of ten days is insufficient to reduce initialization effects to an acceptable degree, although the judgment whether such differences are acceptable can of course not be generalized and depends on a specific application. If differences of 5% or even 10% are acceptable, a ten-day spin up period is sufficient for most species (ozone, CO, VOC, SO_2, NH_4^+ and NH_3) during summer especially when initialized by C-IFS but only for ozone during spring. Spin-up periods of 20 and especially 30 days reduce the differences due to model initialization to less than 1% at a vast majority of grid cells for ozone, CO, VOC, and PAN for the spring and both summer cases. However, for SO_2, NH_3, sulfate, nitrate and ammonium, differences persist at a large number of grid cells even after 30 days during spring and also, though to a lesser extent, during summer. Since all of these species are linked to inorganic aerosol formation, differences in initial conditions for any one of these species can affect all of them. Moreover, since the differences persist for longer than the differences for the ICT, this suggests that this long persistence is not caused by the initial conditions for the atmosphere but rather the initial conditions for the bidirectional NH_3 exchange simulated by CMAQ. This is explored in the following section.

3.2 Soil Concentration Initialization

Unlike most gas phase pollutants, which are consistently deposited, NH_3 can be both emitted from and deposited to land and water surfaces. CMAQ treats this bidirectional surface-air exchange of NH_3 as described in Bash et al. (2010, 2013) and Pleim et al. (2013). The bidirectional exchange model requires information on agricultural management practices and fertilization rates that is provided by running the EPIC model (Williams et al., 1984; 2012) prior to running CMAQ (Cooter et al, 2012). A crucial part of the bidirectional model is the calculation of NH_4^+ and H^+ concentrations in agricultural soil. On the first day of simulation, these values are initialized based on output from the EPIC simulation while on subsequent days, they are calculated directly by the bidirectional model within CMAQ using biogeochemical relationships that mirror those of EPIC for NH_4^+ nitrification with the exception of using the CMAQ modeled time step (approximately 5 minutes for 12 km grid spacing) rather than the larger EPIC time step (daily). CMAQ also differs from EPIC in its parameterization of NH_3 evasion. In CMAQ, the soil NH_3 flux is bidirectional and is a function of the ambient atmospheric NH_3 and sources and sinks of NH_3 in the plant canopy (Pleim et al. 2013; Bash et al., 2013) while EPIC does not consider atmospheric NH_3 concentrations in its NH_3 evasion parameterization. Despite the fact that the bidirectional calculations within CMAQ are similar as the approach implemented in EPIC, differences in simulated soil conditions do exist between EPIC and the bidirectional CMAQ model thus resulting in an initialization effect in the CMAQ calculations on the first day of a simulation.

Figures 5a–d show the differences between the BASE (December 22 initialization) and SPRING_PROF (February 23 initialization) ratios of NH_4^+/H^+ soil concentrations at a depth of 1 cm for March 5, March 15, March 25, April 1, April 11, and April 21. In other words, these maps depict differences in soil conditions 10, 20, 30, 40, 50, and 60 days after the initialization of the SPRING_PROF case. These maps show the largest differences in the

South and Southeast as well as the upper Midwest, but it should be noted that these particular patterns are specific to the time period modeled here since agricultural activity varies both seasonally and spatially. While the differences show a continuous decrease as the length of the simulation increases, they are still noticeable after 30 – 40 days. Qualitatively similar difference maps were found when analyzing the emission potential at a soil depth of 10 cm instead of 1 cm. Time series of air concentration differences were constructed to investigate the impact of these soil concentration differences on atmospheric concentrations of NH_3, inorganic aerosols as well as ozone. Figures 6a–e contain spatially averaged concentrations differences over a range of grid cells that roughly encompass the eastern part of Kansas / Oklahoma, corresponding to an area of large soil concentration differences as shown in Figure 5. The time series for NH_3 concentrations shows differences occasionally exceeding 3 ppb up to 30 days after initialization. The corresponding differences for the inorganic aerosol species are 1 $\mu g/m^3$ for nitrate after 30 days and 0.5 $\mu g/m^3$ for ammonium after roughly 20 days. Note that the differences in the first 5–10 days likely are dominated by initial atmospheric concentration differences discussed in the previous section rather than initial soil concentrations. The results for ozone suggest that the differences in secondary inorganic aerosol formation have only a minor impact on simulated gas phase chemistry, which does not persist for more than 20 days.

It should be noted here that the spring case analyzed above likely represents an upper bound for the persistence of initial conditions for soil NH_4^+ and H^+ because of the dependency of these parameters on agricultural activity and fertilizer use which peak in springtime. Consequently, spin-up periods of more than a month may be necessary if initializing the bidirectional model during springtime but spin-up periods of 30 days should be sufficient for other seasons. This was confirmed by repeating the analysis shown in Figures 5–6 for the summer case. Results of this analysis (not shown here) indicate that a spin-up period of 30 days was sufficient to reduce the effects of soil initialization to negligible levels.

4 Summary

In this study, we investigated the effect of initial conditions for pollutant concentrations in the atmosphere and soil on simulated air quality for two continental-scale CMAQ applications. One of these applications was performed for springtime and the second for summertime. Results show that a spin-up period of ten days commonly used in regional-scale applications may not be sufficient to reduce the effects of initial conditions to less than 1% of seasonally-averaged surface ozone concentrations everywhere while 20 days were found to be sufficient for the entire domain for the spring case and almost the entire domain for the summer case. For the summer case, differences were found to persist longer aloft due to circulation of air masses and even a spin-up period of 30 days was not sufficient to reduce the effects of IC to less than 1% of seasonally-averaged layer 34 ozone concentrations over the southwestern portion of the modeling domain. The results suggest that the effect of using ten-day vs. longer spin-up periods on surface model performance evaluation likely is small, but may be more pronounced for comparisons against upper-air measurements such as ozonesondes. The longer persistence of the effects of initial conditions aloft under certain atmospheric circulation patterns also suggests that spin-up periods need to be carefully considered in studies that are sensitive to simulated free tropospheric concentrations, e.g.

studies aimed at quantifying the effects of lateral boundary conditions on surface ozone since surface ozone has been shown to be more sensitive to lateral boundary conditions originating in upper layers compared to lateral boundary conditions originating in the planetary boundary layer (Baker et al., 2015).

Analysis of the effect of soil initial conditions for the CMAQ bidirectional NH_3 exchange model shows that for the springtime case investigated here they can have an important effect on simulated inorganic aerosols concentrations for time periods of one month or longer. The effects were found to be less pronounced for the summer case considered in this study. Future studies would be needed to quantify the effects of soil initial conditions in other seasons as well as the effects of interannual variability on the persistence of initial conditions.

It needs to be emphasized that the results presented in this study are specific to the modeling domain, year, and time periods simulated here. Smaller modeling domains would likely see less circulation of air masses and therefore less persistence of atmospheric initial conditions but would become more sensitive to lateral boundary conditions. Periods with strong zonal flow patterns that could be present during other seasons or years also likely would require shorter spin-up periods. Despite these caveats, the results nonetheless suggest that modeling protocols need to be scrutinized for a particular application and that it cannot be assumed that commonly-used spin-up periods of three to ten days are necessarily sufficient to reduce the effects of initial conditions on model results to an acceptable level. What constitutes an acceptable level of difference will depend on the particular application, time period and species of interest and cannot be generalized. Moreover, as the application of air quality models is being expanded to cover larger geographical domains and as these models are increasingly being coupled with other modeling systems to better represent air-surface-water exchanges, the effects of model initialization in such applications needs to be studied in future work.

References

Appel KW, Roselle SJ, Gilliam RC, and Pleim JE, 2010 Sensitivity of the Community Multiscale Air Quality (CMAQ) model v4.7 results for the eastern United States to MM5 and WRF meteorological drivers, Geosci. Model Dev, 3, 169–188, doi:10.5194/gmd-3-169-2010

Appel KW, Chemel C, Roselle SJ, Francis XV, Hu R-M, Sokhi RS, Rao ST, Galmarini S, 2012 Examination of the Community Multiscale Air Quality (CMAQ) model performance over the North American and European domains, Atmos. Env, 53, 142–155, 10.1016/j.atmosenv.2011.11.016.

Baker KR, Emery C, Dolwick P, and Yarwood G, 2015 Photochemical grid model estimates of lateral boundary contributions to ozone and particulate matter across the continental United States, Atmos. Env, 123, 49–62, 10.1016/j.atmosenv.2015.10.055

Bash JO, Walker JT, Katul GG, Jones MR, Nemitz E and Robarge WP, 2010 Estimation of in-canopy ammonia sources and sinks in a fertilized Zea mays field, Environ. Sci. Technol 44, 1683–1689 [PubMed: 20104891]

Bash JO, Cooter EJ, Dennis RL, Walker JT, and Pleim JE, 2013 Evaluation of a regional air-quality model with bidirectional NH3 exchange coupled to an agroecosystem model, Biogeosciences, 10, 1635–1645, doi:10.5194/bg-10-1635-2013

Berge E, Huang H-C, Chang J, and Liu T-H, 2001 A study of the importance of initial conditions for photochemical oxidant modeling, J. Geophys. Res, 106, 1347–1363

Brost RA, 1988 The sensitivity of input parameters of atmospheric concentrations simulated by a regional chemical model. J. Geophys Res, 93, 2371–2387, 1988

Byun DW and Schere KL, 2006 Review of the governing equations, computational algorithms, and other components of the Models- 3 Community Multiscale Air Quality (CMAQ) Modeling System, Appl. Mech. Rev, 59, 51–77

Chang JS, Brost RA, Isaksen ISA, Madronich P, Stockwell WR and Walcek CJ, 1987 A three-dimensional eulerian acid deposition model: Physical concepts and formulation, J. Geophys. Res, 92, 14,681–14,700

Cooter EJ, Bash JO, Benson V, and Ran L, 2012 Linking Agricultural Crop Management and Air Quality Models for Regional to National-Scale Nitrogen Assessments. Biogeosciences, 9: 4023–4035. www.biogeosciences.net/9/4023/2012; doi:10.5194/bg-9-4023-2012

Dolwick P, Akhtar F, Baker KR, Possiel N, Simon H, Tonnesen G, 2015 Comparison of background ozone estimates over the western United States based on two separate model methodologies, Atmos. Env, 109, 282–296, 10.1016/j.atmosenv.2015.01.005.

Flemming J, Huijnen V, Arteta J, Bechtold P, Beljaars A, Blechschmidt A-M, Diamantakis M, Engelen RJ, Gaudel A, Inness A, Jones L, Josse B, Katragkou E, Marecal V, Peuch V-H, Richter A, Schultz MG, Stein O, and Tsikerdekis A, 2015 Tropospheric chemistry in the Integrated Forecasting System of ECMWF, Geosci. Model Dev, 8, 975–1003, doi:10.5194/gmd-8-975-2015.

Foley KM, Roselle SJ, Appel KW, Bhave PV, Pleim JE, Otte TL, Mathur R, Sarwar G, Young JO, Gilliam RC, Nolte CG, Kelly JT, Gilliland AB, and Bash JO, 2010 Incremental testing of the Community Multiscale Air Quality (CMAQ) modeling system version 4.7, Geosci. Model Dev, 3, 205–226, doi:10.5194/gmd-3-205-2010.

Gilliam RC, Godowitch JM, and Rao ST, 2012 Improving the horizontal transport in the lower troposphere with four dimensional data assimilation, Atmos. Env, 53, 186–201, doi:10.1016/j.atmosenv.2011.10.064

Giordano L, Brunner D, Flemming J, Hogrefe C, Im U, Bianconi R, Badia A, Balzarini A, Baró R, Chemel C, Curci G, Forkel R, Jiménez-Guerrero P, Hirtl M, Hodzic A, Honzak L, Jorba O, Knote C, Kuenen JJP, Makar PA, Manders-Groot A, Neal L, Pérez JL, Pirovano G, Pouliot G, San José R, Savage N, Schröder W, Sokhi RS, Syrakov D, Torian A, Tuccella P, Werhahn J, Wolke R, Yahya K, Žabkar R, Zhang Y, Galmarini S, 2015 Assessment of the MACC reanalysis and its influence as chemical boundary conditions for regional air quality modeling in AQMEII-2, Atmos. Env, 115, 371–388, 10.1016/j.atmosenv.2015.02.034.

Hogrefe C, Lynn B, Civerolo K, Ku J-Y, Rosenthal J, Rosenzweig C, Goldberg R, Gaffin S, Knowlton K, and Kinney PL, 2004 Simulating changes in regional air pollution over the eastern United States due to changes in global and regional climate and emissions, J. Geophys. Res, 109, D22301, doi:10.1029/2004JD004690

Hogrefe C, Pouliot G, Wong D, Torian A, Roselle S, Pleim J, Mathur R, 2015 Annual application and evaluation of the online coupled WRF–CMAQ system over North America under AQMEII phase 2, Atmos. Env, 115, 683–694, 10.1016/j.atmosenv.2014.12.034.

Pleim JE and Xiu A, 2003 Development of a land surface model. Part II: data assimilation, J. Appl. Meteorol, 42, 1811–1822

Pleim JE and Gilliam R, 2009 An indirect data assimilation scheme for deep soil temperature in the Pleim-Xiu land surface model, J. Appl. Meteorol. Clim, 48, 1362–1376

Pleim JE, Bash JO, Walker JT, and Cooter EJ, 2013 Development and evaluation of an ammonia bidirectional flux parameterization for air quality models, J. Geophys. Res. Atmos, 118, 3794–3806, doi:10.1002/jgrd.50262

Pouliot G, Denier HAC van der Gon, Kuenen J, Zhang J, Moran MD, and Makar PA, 2015 Analysis of the emission inventories and model-ready emission datasets of Europe and North America for phase 2 of the AQMEII project, Atmos. Env, doi:10.1016/j.atmosenv.2014.10.061

Schere K, Flemming J, Vautard R, Chemel C, Colette A, Hogrefe C, Bessagnet B, Meleux F, Mathur R, Roselle S, Hu R-M, Sokhi RS, Rao ST, Galmarini S, 2012 Trace gas/aerosol boundary concentrations and their impacts on continental-scale AQMEII modeling domains, Atmos. Env, 53, 38–50, 10.1016/j.atmosenv.2011.09.043

Sistla G, Hao W, Ku J-Y, Kallos G, Zhang K, Mao H, and Rao ST, 2001 An operational evaluation of two regional-scale ozone air quality modeling systems over the eastern United States, Bull. Am. Meteorol. Soc, 82, 945–964.

Skamarock WC, and Klemp JB, 2007: A time-split nonhydrostatic atmospheric model for research and NWP applications. J. Comp. Phys, special issue on environmental modeling. 3465–3485

Solazzo E, Bianconi R, Hogrefe C, Curci G, Alyuz U, Balzarini A, Baró R, Bellasio R, Bieser J, Brandt J, Christensen J, Colette A, Francis X, Fraser A, Garcia Vivanco M, Jiménez-Guerrero P, Im U, Manders A, Nopmongcol U, Kitwiroon N, Pirovano G, Pozzoli L, Prank M, Sokhi RS, Tuccella P, Unal A, Yarwood G, and Galmarini S: Evaluation and Error Apportionment of an Ensemble of Atmospheric Chemistry Transport Modelling Systems: Multi-variable Temporal and Spatial Breakdown, Atmos. Chem. Phys. Discuss, doi:10.5194/acp-2016-682, accepted for publication in Atmos. Chem. Phys., 2017

Tao Z, Larson SM, Wuebbles DJ, Williams A, and Caughey M, 2003 A summer simulation of biogenic contribution to ground-level ozone over the continental United States, J. Geophys. Res, 108(D14), 4404, doi:10.1029/2002JD002945

Williams JR, Jones CA, and Dyke PT, 1984 A modeling approach to determining the relationship between erosion and soil productivity. Trans. ASAE 27, 129–144

Williams JR, Izaurralde RC and Steglich EM, 2012 Agricultural Policy/Environmental Extender Model, Theoretical Documentation Version 0806, available online at http://apex.tamu.edu/media/72000/the-apex0806-theoretical-documentation.pdf, last accessed November 2, 2016

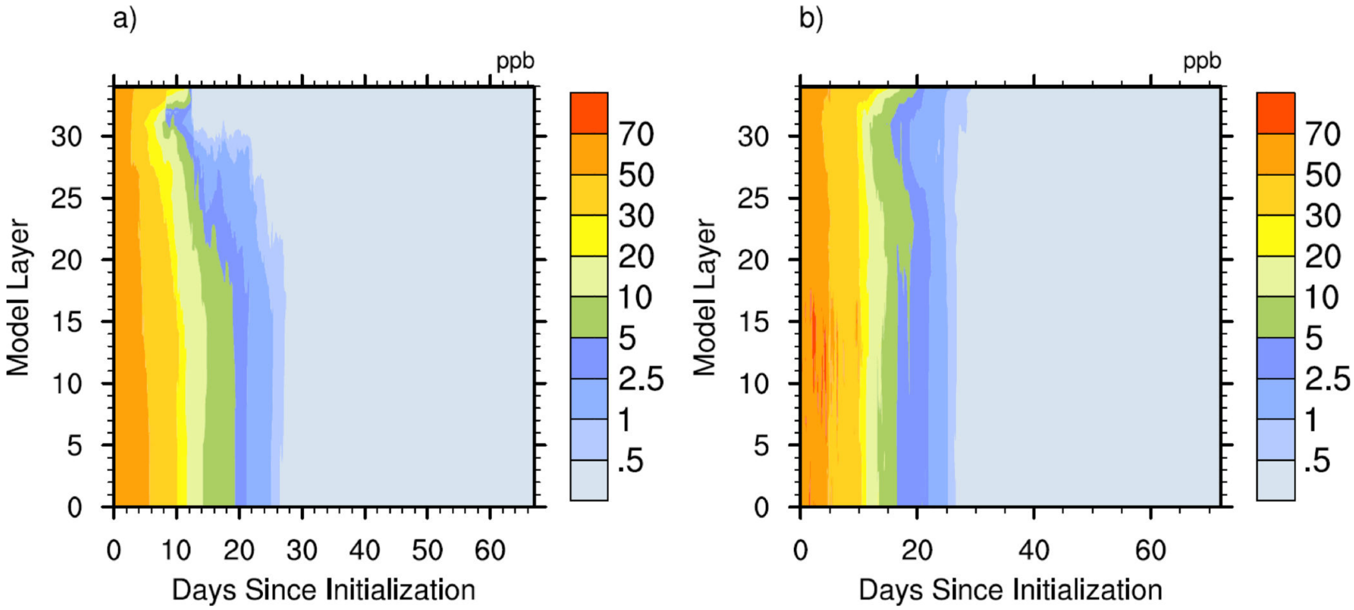

Figure 1a-b.

Time-height cross sections of domain maximum ICT mixing ratios for the a) spring and b) summer cases

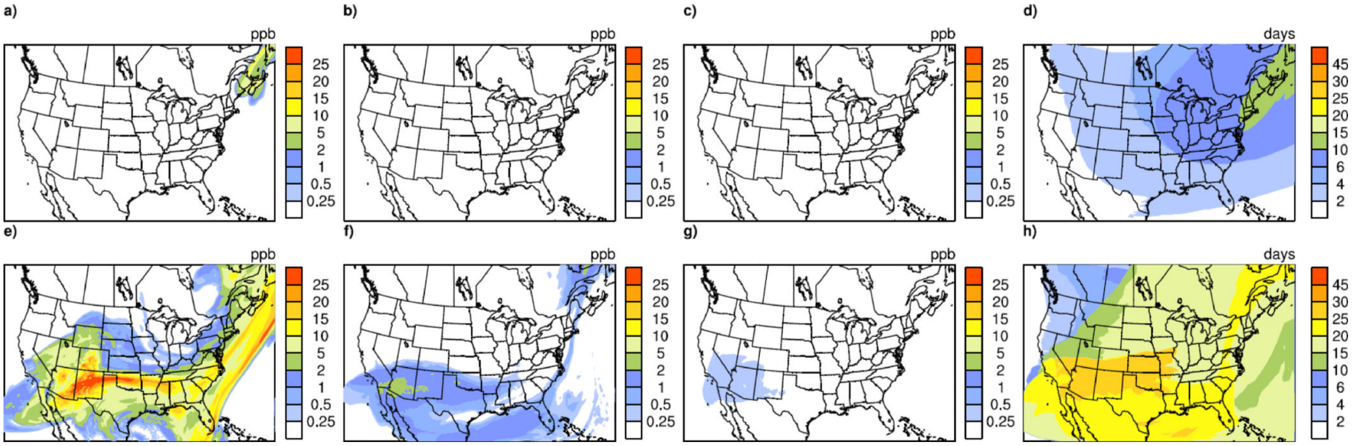

Figure 2.

Panels a-c (e-g) show maps of ICT mixing ratios in model layer 34 after 10, 20 and 30 days for the spring (summer) cases while panels d(h) show maps of the number of days needed for the ICT mixing ratios to drop to below 0.5 ppb (1%) in model layer 34 for the spring(summer) cases.

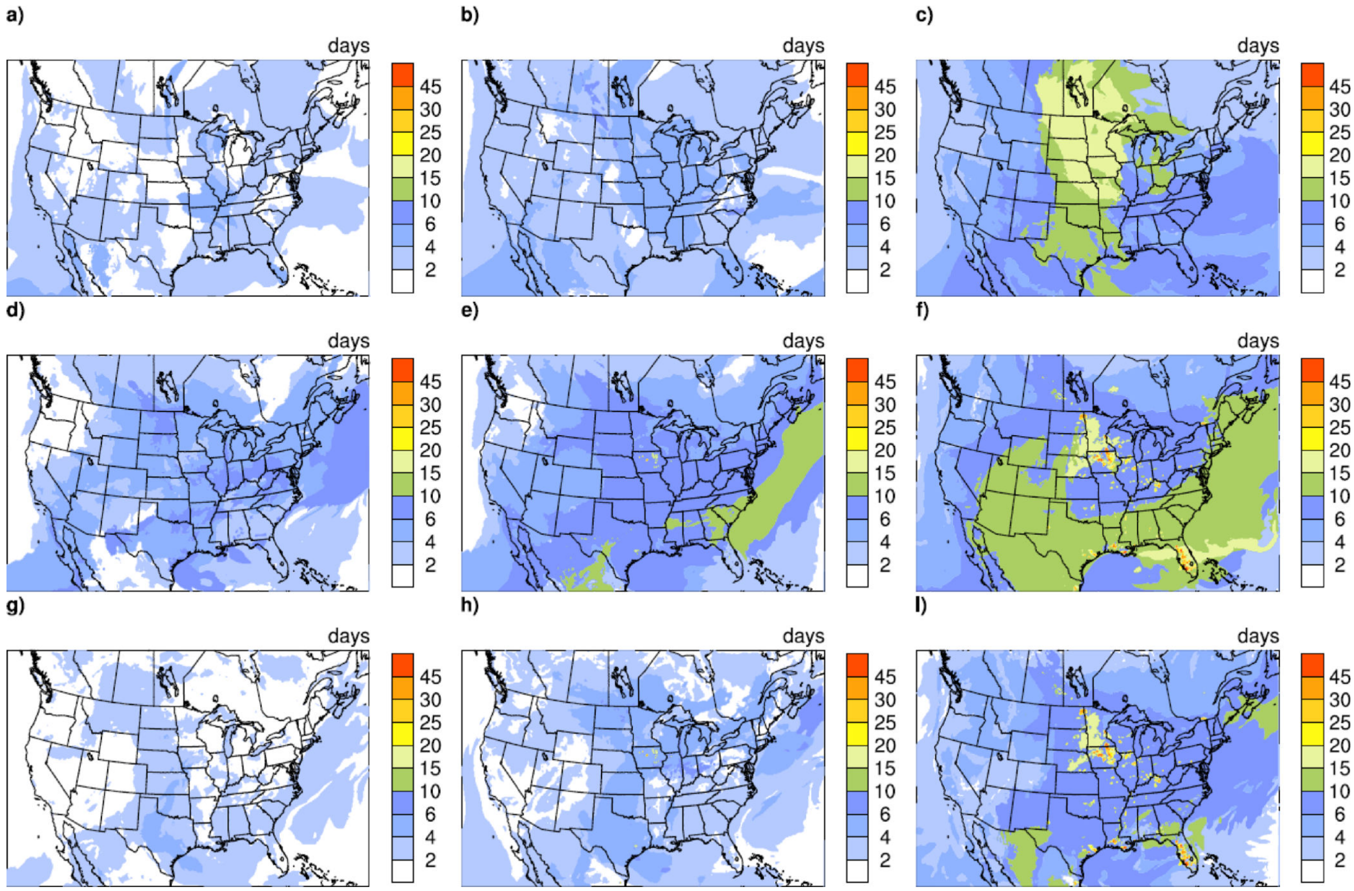

Figure 3.

Figures 3a-c show maps of the number of days needed for differences in daily average ozone concentrations in model layer 1 between the SPRING_PROF and BASE case to drop to below 10%/5%/1% of the grid-cell specific period-average BASE ozone mixing ratio. Figures 3d-f show the corresponding results for the SUMMER_PROF case, and Figures 3g – i show the corresponding results for the SUMMER_CIFS case. Additional details on the computation of the values displayed in the maps are provided in the text.

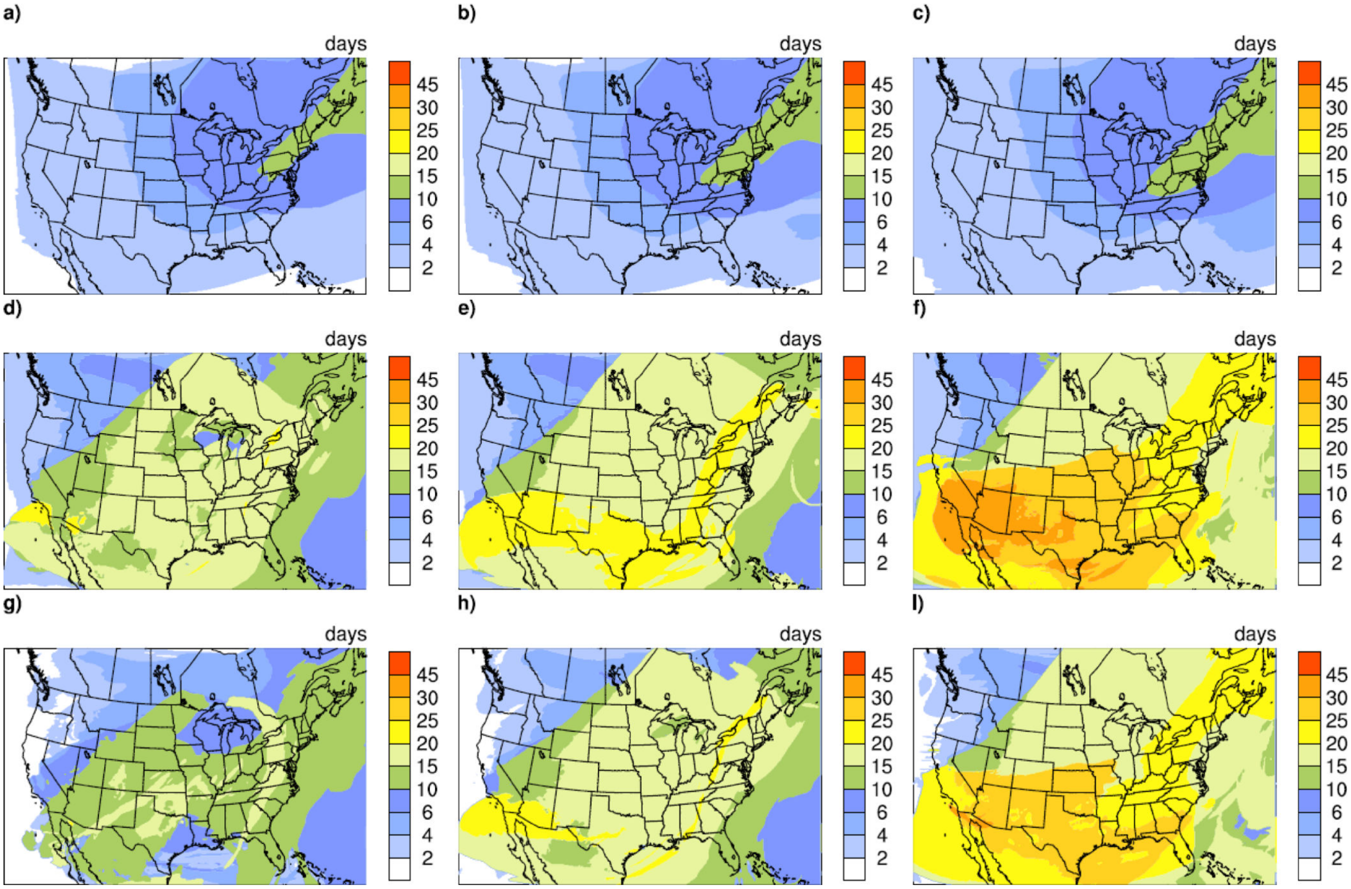

Figures 4.

As in Figure 3 but for model layer 34.

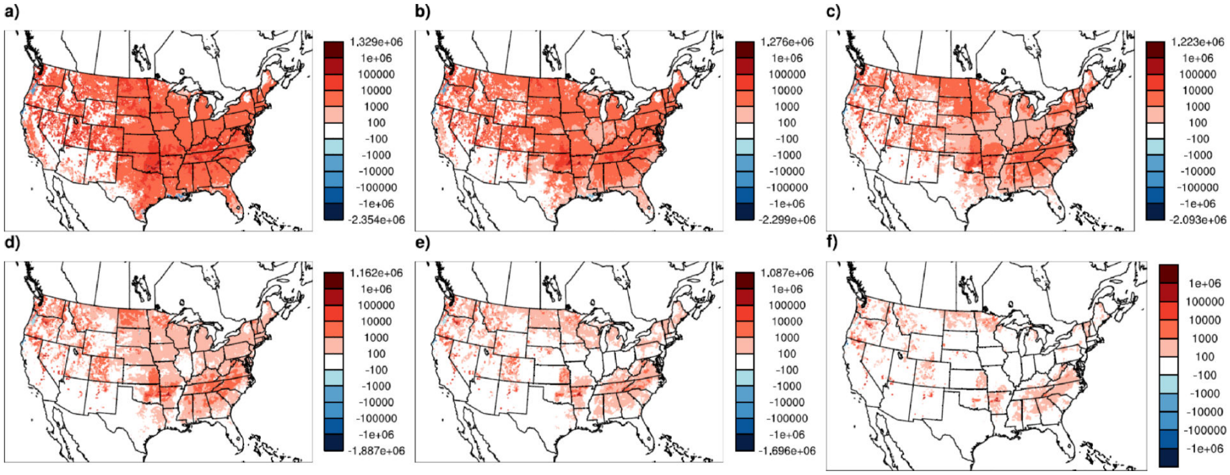

Figure 5:

Map of differences in the ratio of NH_4^+/H^+ soil concentrations (i.e. the emission potential) at a soil depth of 1 cm calculated in the CMAQ bidirectional NH_3 land-surface exchange model on a) March 5, b) March 15, c) March 25, d) April 1, e) April 11, and f) April 21, i.e. 10 days, 20 days, 30 days 40 days, 50 days, and 60 days after initialization for the spring case (February 23). The difference was calculated by subtracting the emission potential for the SPRING_PROF case initialized on February 23 from the emission potential for the BASE case initialized on December 21.

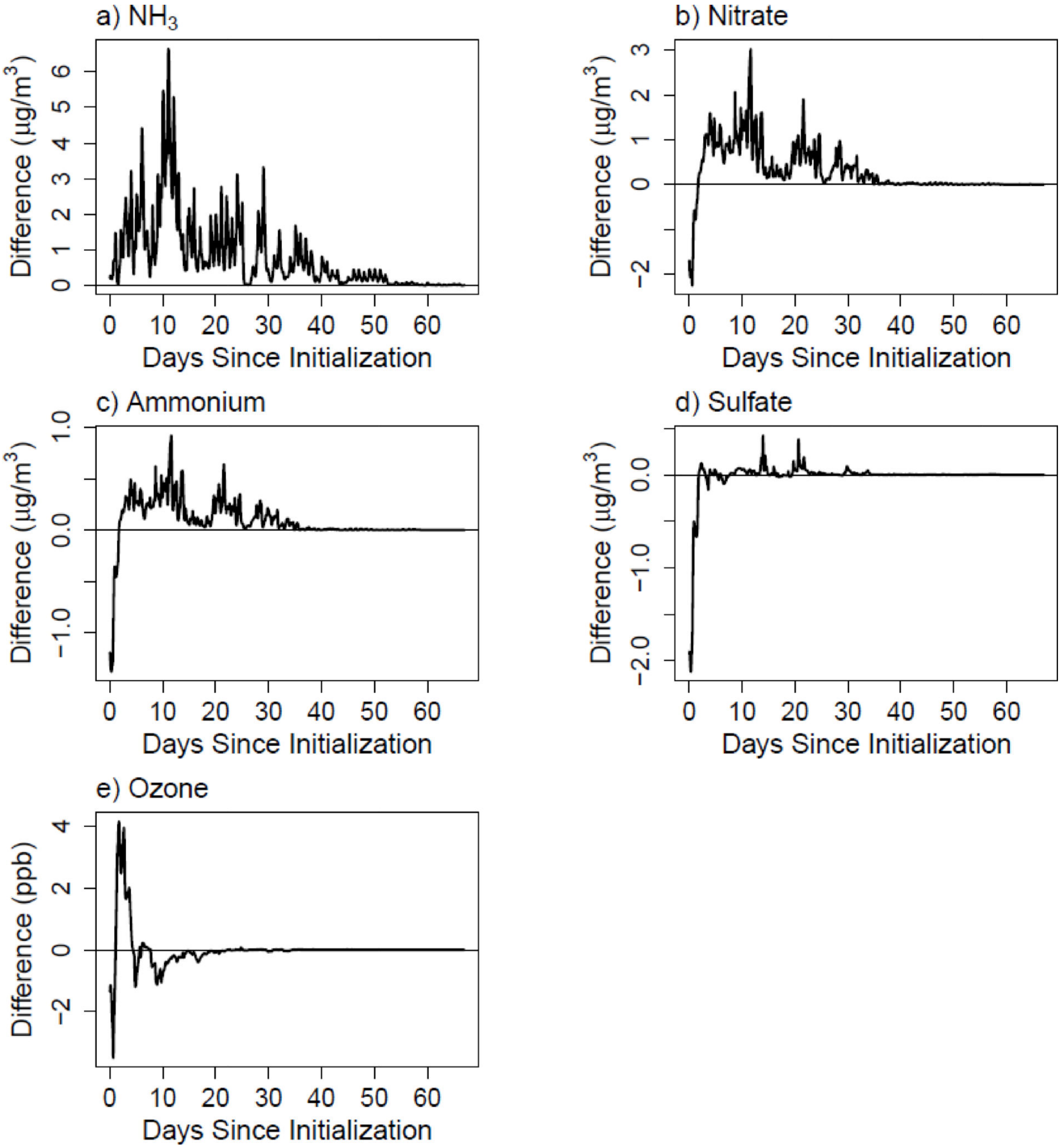

Figure 6.

Time series of atmospheric concentration differences between the two simulations for the spring case, spatially averaged over eastern Kansas and Oklahoma. a) NH_3, b) nitrate, c) ammonium, d) sulfate, and e) ozone. The difference was calculated by subtracting the results for the SPRING_PROF case initialized on February 23 from the results of the BASE case initialized on December 21.

Table 1.

CMAQ default initial conditions for selected species near the surface and at sigma levels 0.45 and 0.15. For a model top at 50 mb and a surface pressure of 1,000 mb, these two sigma levels correspond to approximately 480 mb and 190 mb, respectively.

	O_3 (ppb)	**HNO_3 (ppb)**	**PAN (ppb)**	**CO (ppb)**	**NH_3 (ppb)**	**Sulfate (μg/m^3)**	**Nitrate (μg/m^3)**
Surface	35	0.05	0.02	80	0.1	0.6	0
Sigma level 0.45	60	0.07	0.01	65	0.02	0.08	0
Sigma level 0.15	70	0.1	0	50	0.01	0.04	0

Table 2a.

Number and percentage of grid cells with differences greater than 10%, 5% and 1% of seasonal mean after 10 days of simulation. Results shown are for concentrations in model layer 1.

		O_3	CO	SO2	NH_3	PAN	Nitrate	Ammonium	Sulfate	$PM_{2.5}$
10%	SPRING_PROF	0 (0.0%)	1,788 (2.0%)	117 (0.1%)	28,368 (32.3%)	1,507 (1.7%)	44,834 (51.0%)	35,877 (40.8%)	85 (0.1%)	18,342 (20.9%)
	SUMMER_PROF	0 (0.0%)	0 (0.0%)	86 (0.1%)	3,753 (4.3%)	1,717 (2.0%)	3,009 (3.4%)	32 (0.0%)	0 (0.0%)	0 (0.0%)
	SUMMER_CIFS	0 (0.0%)	0 (0.0%)	0 (0.0%)	3,337 (3.8%)	2 (0.0%)	3,621 (4.1%)	9 (0.0%)	0 (0.0%)	0 (0.0%)
5%	SPRING_PROF	0 (0.0%)	12,178 (13.9%)	1,769 (2.0%)	36,001 (41.0%)	11,619 (13.2%)	50,855 (57.9%)	46,133 (52.5%)	927 (1.1%)	28,973 (33.0%)
	SUMMER_PROF	1,322 (1.5%)	7,858 (8.9%)	229 (0.3%)	10,448 (11.9%)	8,161 (9.3%)	6,757 (7.7%)	295 (0.3%)	42 (0.0%)	7 (0.0%)
	SUMMER_CIFS	3 (0.0%)	0 (0.0%)	10 (0.0%)	9,612 (10.9%)	1,707 (1.9%)	7,743 (8.8%)	291 (0.3%)	0 (0.0%)	3 (0.0%)
1%	SPRING_PROF	13,924 (15.9%)	36,829 (41.9%)	13,685 (15.6%)	50,685 (57.7%)	30,017 (34.2%)	58,614 (66.7%)	60,535 (68.9%)	25,919 (29.5%)	49,827 (56.7%)
	SUMMER_PROF	17,293 (19.7%)	32,999 (37.6%)	2,639 (3.0%)	38,933 (44.3%)	25,847 (29.4%)	27,073 (30.8%)	12,086 (13.8%)	8,898 (10.1%)	13,330 (15.2%)
	SUMMER_CIFS	661 (0.8%)	10,840 (12.3%)	1,079 (1.2%)	35,897 (40.9%)	17,106 (19.5%)	27,902 (31.8%)	19,808 (22.6%)	15,243 (17.4%)	6,554 (7.5%)

Table 2b.

Number and percentage of grid cells with differences greater than 10%, 5% and 1% of seasonal mean after 20 days of simulation. Results shown are for concentrations in model layer 1.

		O_3	CO	SO2	NH_3	PAN	Nitrate	Ammonium	Sulfate	$PM_{2.5}$
10%	SPRING_PROF	0 (0.0%)	0 (0.0%)	75 (0.1%)	18,186 (20.7%)	0 (0.0%)	28,130 (32.0%)	22,968 (26.1%)	216 (0.2%)	2,893 (3.3%)
	SUMMER_PROF	0 (0.0%)	0 (0.0%)	0 (0.0%)	34 (0.0%)	3 (0.0%)	183 (0.2%)	1 (0.0%)	0 (0.0%)	0 (0.0%)
	SUMMER_CIFS	0 (0.0%)	0 (0.0%)	0 (0.0%)	33 (0.0%)	3 (0.0%)	191 (0.2%)	3 (0.0%)	0 (0.0%)	0 (0.0%)
5%	SPRING_PROF	0 (0.0%)	0 (0.0%)	1,157 (1.3%)	32,072 (36.5%)	0 (0.0%)	37,662 (42.9%)	34,302 (39.1%)	1,088 (1.2%)	11,779 (13.4%)
	SUMMER_PROF	0 (0.0%)	0 (0.0%)	0 (0.0%)	207 (0.2%)	54 (0.1%)	601 (0.7%)	1 (0.0%)	0 (0.0%)	0 (0.0%)
	SUMMER_CIFS	0 (0.0%)	0 (0.0%)	0 (0.0%)	199 (0.2%)	55 (0.1%)	606 (0.7%)	7 (0.0%)	0 (0.0%)	0 (0.0%)
1%	SPRING_PROF	0 (0.0%)	0 (0.0%)	10,534 (12.0%)	62,944 (71.7%)	355 (0.4%)	52,702 (60.0%)	50,657 (57.7%)	16,424 (18.7%)	39,526 (45.0%)
	SUMMER_PROF	166 (0.2%)	0 (0.0%)	0 (0.0%)	3,480 (4.0%)	989 (1.1%)	3,652 (4.2%)	294 (0.3%)	1 (0.0%)	20 (0.0%)
	SUMMER_CIFS	168 (0.2%)	0 (0.0%)	0 (0.0%)	3,414 (3.9%)	976 (1.1%)	3,670 (4.2%)	298 (0.3%)	1 (0.0%)	27 (0.0%)

Table 2c.

Number and percentage of grid cells with differences greater than 10%, 5% and 1% of seasonal mean after 30 days of simulation. Results shown are for concentrations in model layer 1.

		O_3	CO	SO2	NH_3	PAN	Nitrate	Ammonium	Sulfate	$PM_{2.5}$
10%	SPRING_PROF	0 (0.0%)	0 (0.0%)	0 (0.0%)	12,814 (14.6%)	0 (0.0%)	18,411 (21.0%)	8,392 (9.6%)	31 (0.0%)	1,071 (1.2%)
	SUMMER_PROF	0 (0.0%)	0 (0.0%)	0 (0.0%)	2 (0.0%)	0 (0.0%)	75 (0.1%)	2 (0.0%)	0 (0.0%)	0 (0.0%)
	SUMMER_CIFS	0 (0.0%)	0 (0.0%)	0 (0.0%)	2 (0.0%)	0 (0.0%)	84 (0.1%)	1 (0.0%)	0 (0.0%)	0 (0.0%)
5%	SPRING_PROF	0 (0.0%)	0 (0.0%)	12 (0.0%)	24,214 (27.6%)	0 (0.0%)	27,196 (31.0%)	18,439 (21.0%)	765 (0.9%)	7,835 (8.9%)
	SUMMER_PROF	0 (0.0%)	0 (0.0%)	0 (0.0%)	10 (0.0%)	0 (0.0%)	163 (0.2%)	3 (0.0%)	0 (0.0%)	0 (0.0%)
	SUMMER_CIFS	0(0.0%)	0 (0.0%)	0 (0.0%)	8 (0.0%)	0 (0.0%)	179 (0.2%)	2 (0.0%)	0 (0.0%)	0 (0.0%)
1%	SPRING_PROF	0 (0.0%)	0 (0.0%)	5,718 (6.5%)	46,761 (53.2%)	0 (0.0%)	42,740 (48.7%)	38,985 (44.4%)	9,491 (10.8%)	24,845 (28.3%)
	SUMMER_PROF	51 (0.1%)	0 (0.0%)	1 (0.0%)	67 (0.1%)	124 (0.1%)	1,005 (1.1%)	54 (0.1%)	0 (0.0%)	5 (0.0%)
	SUMMER_CIFS	51 (0.1%)	0 (0.0%)	0 (0.0%)	67 (0.1%)	123 (0.1%)	1,095 (1.2%)	65 (0.1%)	0 (0.0%)	6 P(0.0%)